Neural Networks 87 (2017) 27–37

Contents lists available at ScienceDirect

Neural Networks

journal homepage: www.elsevier.com/locate/neunet

Cognitive memory and mapping in a brain-like system for robotic navigation

Huajin Tang [a], Weiwei Huang [b], Aditya Narayanamoorthy [b], Rui Yan [a,*]

[a] Neuromorphic Computing Research Center, College of Computer Science, Sichuan University, Chengdu, 610065, China
[b] Institute for Infocomm Research, Agency for Science Technology and Research (A*STAR), Singapore 138632, Singapore

ARTICLE INFO

Article history:
Received 12 February 2015
Received in revised form 1 July 2016
Accepted 4 August 2016
Available online 7 December 2016

Keywords:
Hippocampus
Entorhinal cortex
Brain-like system
Spatial cognition
Navigation
Neurorobotics

ABSTRACT

Electrophysiological studies in animals may provide a great insight into developing brain-like models of spatial cognition for robots. These studies suggest that the spatial ability of animals requires proper functioning of the hippocampus and the entorhinal cortex (EC). The involvement of the hippocampus in spatial cognition has been extensively studied, both in animal as well as in theoretical studies, such as in the brain-based models by Edelman and colleagues. In this work, we extend these earlier models, with a particular focus on the spatial coding properties of the EC and how it functions as an interface between the hippocampus and the neocortex, as proposed by previous work. By realizing the cognitive memory and mapping functions of the hippocampus and the EC, respectively, we develop a neurobiologically-inspired system to enable a mobile robot to perform task-based navigation in a maze environment.

1. Introduction

The autonomous capabilities of robots and learning systems, for example, autonomous navigation through brain cognitive functions, have attracted increasing interest (Edelman, 2007; Fleischer & Edelman, 2009; Shim, Ranjit, Tian, Yuan, & Tang, 2015; Wyeth & Milford, 2009). Navigating in a complex world is an effortless task for humans, yet it is still a challenging problem in the robotics area (Dissanayake, Newman, Clark, Durrant-Whyte, & Csorba, 2001; Shim, Tian, Yuan, Tang, & Li, 2014; Tian et al., 2013). Many models such as Kalman filters (Thrun, Burgard, & Fox, 2005) and Particle filters (Montemerlo & Thrun, 2003) are used to build a practical and robust Simultaneous Localization And Mapping (SLAM) algorithm. SLAM is a cartographic method providing metric map and current location for the navigation system.

Animals such as rat and primates have an inborn ability to form spatial representations in a highly dynamic and extensive environment, while simultaneously navigating it. Neurophysiological studies suggest that the hippocampus, together with the entorhinal cortex (EC), plays an important role in memory and spatial cognition (Cheu, Yu, Tan, & Tang, 2012; Frank, Brown, & Wilson, 2000; Tang, Li, & Yan, 2010). In 1971, O'Keefe found the "place cell" property of the hippocampus in rodent experiments (O'Keefe & Dostrovsky, 1971). A "place cell" has a high firing rate when the rodent is in a particular location within its environment (O'Keefe & Nadel, 1978).

At a macroscopic level, highly processed neocortical information from all sensory inputs converges onto the medial temporal lobe (MTL) where the hippocampus resides (Lavenex & Amaral, 2000). These processed signals enter the hippocampus via the EC. Within the hippocampus, there are connections from the EC to all fields of the hippocampal formation, including the dentate gyrus (DG), CA3 and CA1 (Amaral, Ishizuka, & Claiborne, 1990; Bernard & Wheal, 1994; Treves & Rolls, 1994).

With regards to hippocampal models, Barrera and Weitzenfeld (2006) proposed a neural structure to mimic the "place field" property of the hippocampus and guide a robot in searching for a goal. More recent work shows that the dorsocaudal medial entorhinal cortex (dMEC) is considered to have a neural representation of the layout of the environment (Fyhn, Molden, Witter, Moser, & Moser, 2004; O'Keefe & Nadel, 1978). The key units are identified as "grid cells" (Hafting, Fyhn, Molden, Moser, & Moser, 2005). McNaughton, Battaglia, Jensen, Moser, and Moser (2006) suggested an attractor network structure to demonstrate the path integration for the cognitive map in dMEC. Similarly, Wyeth and Milford (2009) implemented a 3-dimensional continuous attractor network (CAN) to simulate the map-like structure in the EC. In our recent neuro-robotic experimental

* Corresponding author.
E-mail address: ryan@scu.edu.cn (R. Yan).

http://dx.doi.org/10.1016/j.neunet.2016.08.015
0893-6080/

studies, we have revealed that cognitive map building is a process integrating responses from both the grid cells and the place cells in the EC-Hippocampal area (Yuan, Tian, Shim, Tang, & Li, 2015), and that the enhanced visual features play an important role in hippocampal spatial responses, and thus in spatial cognition in a simulated robotic platform (Huang, Tang, & Tian, 2014).

Based on the connection properties of subregions in the hippocampus, Edelman and colleagues (Edelman, 2007; Fleischer & Edelman, 2009; Krichmar, Nitz, Gally, & Edelman, 2004) developed a brain-based device (BBD) to understand the mechanisms of how the vertebrate nervous system gives rise to cognition and behavior. Many interesting properties such as "place cells" and "episodic memory" in the hippocampus have been realized with this model. In the BBD model, the EC functions as interface between the neocortex and the hippocampus. However, focus on the coding of goal location – an important feature of the EC – is not that high in previous studies.

In this paper, inspired by previous work on explaining the rat's navigation and on brain-inspired navigation models, we develop a brain-like cognitive model and apply it to robotic spatial cognitive tasks. In our system, the general architecture is inherited from the BBD model developed by Edelman's group (Edelman, 2007). As opposed to their previous studies, we focus on the realization of the spatial mapping property of the EC area, and how this can be used to encode task goal locations. All the connections in our model from the hippocampus to other cortical areas are connected via the EC. Treves and Rolls (1994) initially proposed this structure, which was then further supported in Lavenex and Amaral's work (Lavenex & Amaral, 2000). Their studies suggest that the EC does not merely act as a relay for the flow of information from cortical areas to the hippocampal complex, but participates actively in the memory processes, especially in spatial memory (Fyhn et al., 2004; Lavenex & Amaral, 2000). One important feature of these previous works is that the EC is considered as a neural mapping of the spatial environment. In the navigation tasks with this model, when a robot recognizes an image it has seen before – using information stored in the CA1 region of the hippocampus – the associated location information stored in the EC is retrieved concurrently, since both these fields are connected. Hence, with this neural system, the robot can use its mapping and navigation abilities to perform cognitive tasks. These tasks are encoded such that the user can specify both solitary as well as multiple tasks to our trained model.

2. Methodology

2.1. System structure

2.1.1. Neural structure

Inspired by the BBD model, the schematic of our neural structure is shown in Fig. 1. Overall, the neural architecture includes three layers: the Neocortex, the EC and the Hippocampus.

The neocortex in our brain-inspired model contains three cortical regions: IT, ANT and Mhdg, which correspond to the inferotemporal cortex, the anterior nucleus of thalamus and a motor cortical area (Fleischer & Edelman, 2009). The inputs to the neocortex, which feed in information from the environment, come from a camera and a compass. The visual information is divided into two regions: V1shape and V1color, which represent the shape and color information, respectively. The corresponding value is calculated through an HMAX algorithm (Riesenhuber & Poggio, 1999) (described in detail in Section 2.1.3) and a color filter, respectively. The compass value is used to model the head direction (HD) neural area; 360 neurons are used to encode a heading direction between 0 and 359°. Each neuron has a cosine

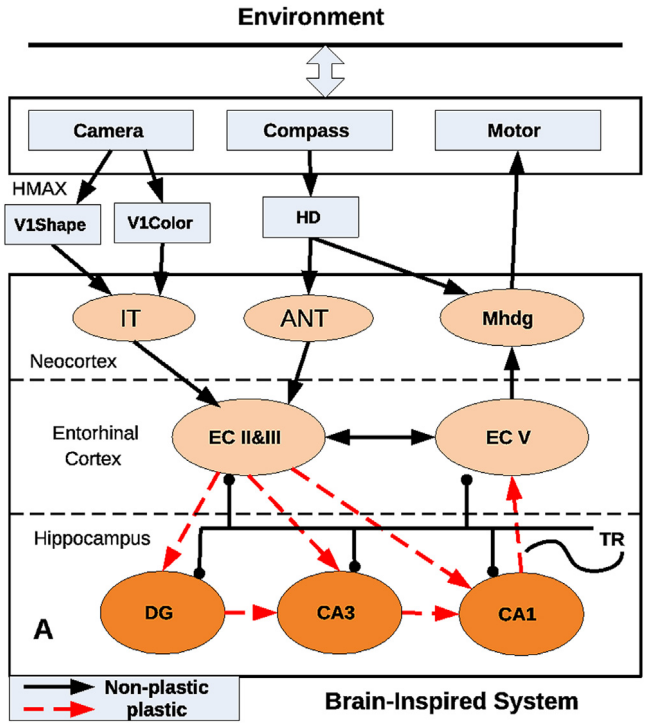

Fig. 1. Schematic of the regional and functional neuroanatomy of the brain-based neural system. Ellipses denote different neural areas; boxes denote different devices; arrows denote projections from one area to another. Inputs to the neural system come from a camera and a compass; the image information is projected to the inferotemporal cortex (IT) through an HMAX process and a color filter; the orientation information is projected to the anterior nucleus of thalamus (ANT). The entorhinal cortex (EC) functions as the interface between the hippocampus and the neocortex, consisting of two parts — ECII&III and ECV. The output from ECV goes to a motor cortical area (Mhdg), which maps onto a motor that dictates the movement of the robot. Inside the hippocampus, there are cortical areas including the dentate gyrus (DG), CA3 and CA1. A theta rhythm (TR) signal is used to inhibit the hippocampal area, to keep activity levels stable. In this neuron design, each cortical region has a twin inhibition component to maintain stability. To simplify the figure, these inhibition components are not shown. The detailed parameters of these inhibition components are given in Appendix A. (For interpretation of the references to color in this figure legend, the reader is referred to the web version of this article.)

tuning curve to respond to a preferred heading. The tuning curve is described as follows:

$$HD_i = \cos\left(\frac{i}{360}2\pi - HD_C\right)^{11} \tag{1}$$

where HD_i is the ith neuron's activity with a preferred direction of i degrees; HD_C is the compass input in radius. The head direction neurons are mapped to the anterior nucleus of thalamus (ANT) and to the motor neuron area. The output of this cortical area is to the Mhdg, which dictates the moving direction of the robot. It consists of 60 neurons correspond to heading from 0 to 359°, i.e. each neuron corresponds to a moving range of 6°. The motor neuron with the strongest activity will determine the direction of movement.

The EC is the main interface between the hippocampus and the neocortex. It receives highly processed inputs from every sensory module. The EC is responsible for the pre-processing of the input signals. Biologically, the superficial layers, including layers II and III, project to the hippocampus. Layer II primarily projects to the DG and CA3 cortical areas in the hippocampus. Layer III primarily projects to the CA1 area in the hippocampus. The deep layer, layer V, receives one of three outputs from the hippocampus and reciprocates connections from cortical areas that project to the superficial EC (Hargreaves, Rao, Lee, & Knierim, 2005). To simplify

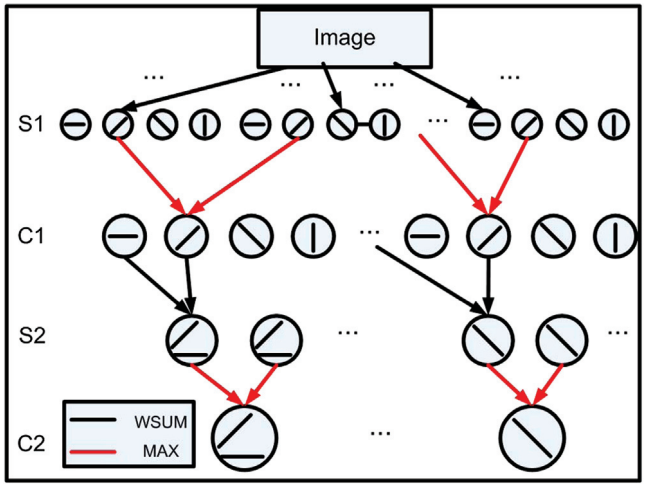

Fig. 2. HMAX model for the object recognition (Riesenhuber & Poggio, 1999). The circuitry consists of a hierarchy of layers of visual processing that use two different types of pooling method: weighted sum (WSUM) and maximum (MAX). The first layer S1 performs a linear-oriented filter and normalization to the input image. In the next layer C1, outputs of S1 with same orientation that are located close to each other are selected by a maximum operation. In the stage S2, outputs from C1 in locations that are close by are combined to form more complex features. The C2 layer is similar to C1 layer: by pooling together outputs of S2 that are near each other and have the same type using a maximum operation. The output of the C2 layer is mapped to the IT as in a ventral cortical pathway.

our model, we combine layer II and layer III together as the input layer; layer V is designed as the goal location encoder of the spatial environment.

The EC connects inputs from all the sensory regions to all fields of the hippocampal formation, including DG, CA3 and CA1 through perforant pathways. The DG connects with CA3 through mossy fibers. The CA3 connects with CA1 through schaffer collaterals, and the CA1 connects back to the EC output (ECV in our model). There are also strong recurrent connections within CA3.

In Fig. 1, most of the neural regions in the neocortex, EC and hippocampus are designed with a corresponding inhibition component (ITi, ANTi, Mhdgi, ECII&IIIi, ECVi, DGi, CA3i and CA1i). These inhibition components have the same neuron size as their excitation parts (IT, ANT, Mhdg, ECII&III, ECV, DG, CA3 and CA1). They receive inputs from the excitation regions. In return, they inhibit these regions to maintain their stability. For brevity, these inhibition components are not included in Fig. 1. The detailed connections between all regions is given in Appendix A.

2.1.2. Information flow

The system interacts with the environment through various sensors. In this design, the sensors include a camera and a compass which function as eyes, and magnetite in the ethmoid bone, respectively. These sensory signals are encoded to neural signals in the neocortex. Then, these signals are combined together in the EC. The neuronal activities of the EC form a corresponding response to the current environment. In the hippocampus, this pattern of response is memorized and can be retrieved when a hint input is later provided.

When the memory is recalled, it activates the corresponding response in the EC output layer. The memory is decoded here. For example, in a navigation application, the memory information stored in the hippocampus can be translated into a location that the robot has memorized before. In this case, the decoding of the EC output layer functions as a map corresponding to the spatial environment. The map information in the EC output layer projects to the motor cortical area according to the desired task. The motor cortical area decodes the neural commands from the EC output layer and sends these to the corresponding actuators that move the robot.

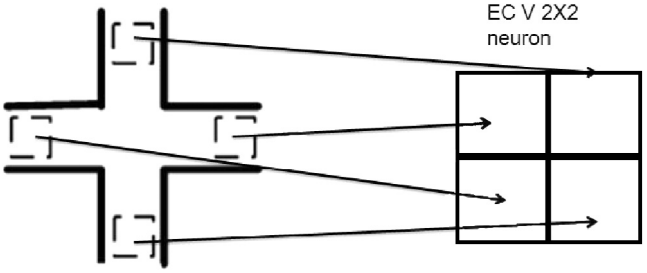

Fig. 3. The mapping of locations in the plus-maze to ECV neurons; i.e. the East location corresponds to neuron (1, 1), North corresponds to (1, 2), West corresponds to (2, 1) and South corresponds to (2, 2).

2.1.3. Hierarchical vision architecture

Visual information in the visual cortex is considered to be processed through ventral visual pathway (Ungerleider & Haxby, 1994) running from the primary visual cortex (V1) over extrastriate visual areas V2 and V4 to the inferotemporal cortex (IT). It is classically modeled as a hierarchically-layered structure. Here, we adopt the HMAX hierarchical vision architecture which is a computational model of object recognition in the visual cortex. As shown in Fig. 2, the HMAX model consists of four layers with linear and non-linear operations. The first layer, namely S1, performs a linear-oriented filter and normalization to the input image. In the next layer (C1), outputs of S1 with same orientation which are near each other are selected by a maximum operation. In the next stage (S2), outputs from C1 which are near each other are combined to form more complex features. The C2 layer is similar to C1 layer: those nearby outputs of S2 having the same type are pooled together by a maximum operation. The information in C2 becomes more invariant to position and scale, but preserves feature selectivity, which may correspond roughly to the V4 area in the visual cortex (Riesenhuber & Poggio, 1999). The output of the C2 layer is mapped to the inferotemporal cortex (IT), as in the ventral cortical pathway (HMAX $\rightarrow$ IT).

2.1.4. Neural structure of EC

The EC in our model represents a neural mapping of the spatial environment. To test this property, each neuron in ECV is mapped to a spatial location. In our experiments in a plus-maze environment, each arm of the plus maze is mapped to a neuron group in ECV, as shown in Fig. 3. Due to the simplicity of the environment, only four neurons are required to represent the plus-maze environment.

2.1.5. Task encoding and learning method

Similar to how the ECV region encodes locations, there is another neural region called the Task region. It is connected to neurons in the EC as a one-to-one mapping. Each Task neuron represents a request to the robot to move to the associated location in ECV, and is made to fire either when the user wishes to associate a location in ECV with a set of input while training, or when the user wishes to give these encoded locations as goals to a trained robot. For both these purposes, different strengths of input are used to the Task region. While training, a larger value is used, to potentiate the corresponding ECV neuron enough, so that it associates that neuron with the given input to the system. During testing, a smaller value of input to the Task neuron is given; this, combined with the right sensory input to the system, potentiates the corresponding ECV neuron to a greater extent. Further details on this neural region are described in Appendix A, section B.

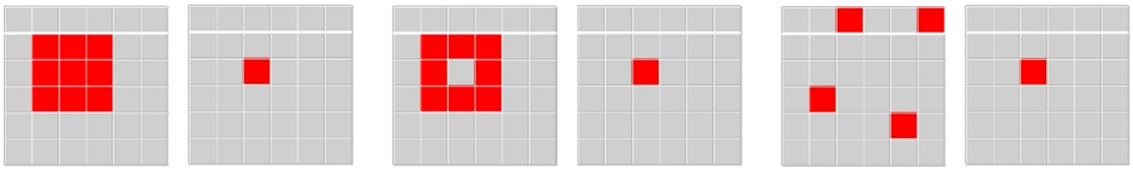

(A) Rectangular []3 × 3. (B) Doughnut $\theta 1 \times 2$. (C) Nontopo.

Fig. 4. Different connection types between neural regions. The right side of each connection shows the field being connected to, while the left side shows the target neuronal units that are connected. (A) Neurons connected are described by a rectangle centered on the current neuron, with a specified width and height. (B) Neurons connected are described by concentric circles centered on the current neuron, with specified inner and outer radii. (C) Neurons connected are chosen at random.

2.2. Properties of the simulated neural system

2.2.1. Neural dynamics

In our neural system, all neuronal units are described by a mean firing rate model. The mean firing rate range of each neuronal unit varies from 0 (no firing) to 1 (maximal firing). The state of a neuronal unit is calculated based on its current state and contributions from other neuronal units. The postsynaptic influence on unit i is calculated based on the equation:

$$Post_i(t) = \sum_{j=1}^{M} [w_{ij} s_j(t)] \tag{2}$$

where $s_j(t)$ is the activity of unit j; w_{ij} is the connection strength from unit j to unit i; M is the number of connections to unit i.

The new activity is determined by the following activation function:

$$s_i(t+1) = \Phi(\tanh(g_i Post_i(t) + \omega s_i(t))) \tag{3}$$

$$\Phi(x) = \begin{cases} 0 & x < \delta_i^{fire} \\ x & \text{otherwise} \end{cases} \tag{4}$$

where g_i is the scaling factor; ω controls the persistence of unit activity from the previous state; δ_i^{fire} is the firing threshold.

2.2.2. Neural connections

The ways in which different neural regions connect together are divided into three types. The first type is "rectangular" with a given height and width "h × w" as shown in Fig. 4(A). The second type is "doughnut" with an inner and outer radius "$\Theta r1 \times r2$", excluding the center as shown in Fig. 4(B). The third type is called "nontopo" in which any pair of presynaptic and postsynaptic neurons have an equal probability of being connected as shown in Fig. 4(C).

2.2.3. Neural plasticity

In learning and memory systems, synaptic plasticity is one of the key ways in which the neural network learns and stores memory (Martin, Grimwood, & Morris, 2000). Experimental data from the visual cortex led to a synaptic modification rule, namely the BCM rule. The rule has two main features: (1) synapses between neuronal units with strongly correlated firing rates are potentiated; (2) a synaptic modification threshold for each neuron which controls the direction of weight modification. In this paper, the synaptic plasticity is based on a modified BCM learning rule (Fleischer & Krichmar, 2007):

$$\Delta w_{ij}(t+1) = \eta s_i(t) s_j(t) BCM(s_i(t)) \tag{5}$$

$$BCM(s) = \begin{cases} -k_1 s & s \le \dfrac{\Theta}{2} \\ k_1(s - \Theta) & \dfrac{\Theta}{2} > s \le \Theta \\ k_2 \tanh(6(s - \Theta))/6 & \text{otherwise} \end{cases} \tag{6}$$

where $s_i(t)$ and $s_j(t)$ are activities of postsynaptic and presynaptic units, respectively; η is the learning rate; k_1 and k_2 are the two inclinations. The threshold Θ is adjusted based on the postsynaptic activity:

$$\Delta\Theta = 0.25(s_i^2(t) - \Theta). \tag{7}$$

2.2.4. Theta rhythm inhibition

In the system structure, a theta rhythm (TR) signal is used to inhibit neural regions to keep activity level stable (TR → ECII&III, ECV, DG, CA3, CA1). The TR activity follows a half cycle of sinusoidal wave:

$$TR(n) = \sin\left(\text{mod}\left(\frac{n\pi}{N}, \pi\right)\right) \tag{8}$$

where n is the time step; N is the number of steps that are required for the hippocampus to reach a stable state for a new input.

2.2.5. Parameter values

All parameters used in the above equations are listed out in Appendix A. The Task region, not being a regular neural region, has different parameters, given in Appendix B.

2.3. Key features of the system

2.3.1. Learning visual inputs

In our cognitive neural system, the HMAX model and color filter are employed to generate the key information of the input images. The EC processes this vision information and passes it to the hippocampal regions, including DG, CA3 and CA1. As discussed in earlier work in this field (Kesner, Lee, & Gilbert, 2004), DG plays the role of capturing the abstract information from EC area through a competitive computation mechanism. To have this function, the self-inhibition of DG is very strong (as shown by parameter values for connections between DG and its inhibitory region, in Table 2 under Appendix A). It inhibits more surrounding neurons in comparison to the self-inhibition in CA3 and CA1 areas. Due to this competitive learning process, the key information from the EC remains in the DG. The CA3 serves to store the memory information in the hippocampus. In our design, a strong recurrent connection is included in the CA3 region (Table 2 under Appendix A). This enables the CA3 to form a stable pattern for a given input. The stabilized response of CA3 will then activate the corresponding pattern in CA1. The stabilized pattern in CA1 is associated with the sensory inputs.

Fig. 5 shows a result of an auto-association experiment performed in a previous work (Huang et al., 2014). When training, the desired result is directly fed into the output region (ECV), so that the plastic connections within the model learn to associate the input and desired output. One cycle of training consists of showing the input image for one theta cycle (as determined by N in Eq. (8)), which allows the response of the neural regions to stabilize. After two such cycles of training, the plastic connections within the hippocampal regions and to the output neuronal region are sufficiently modified, so the neural system, on being presented with the input image again, can recall the output pattern by itself and show it in the output neuronal area.

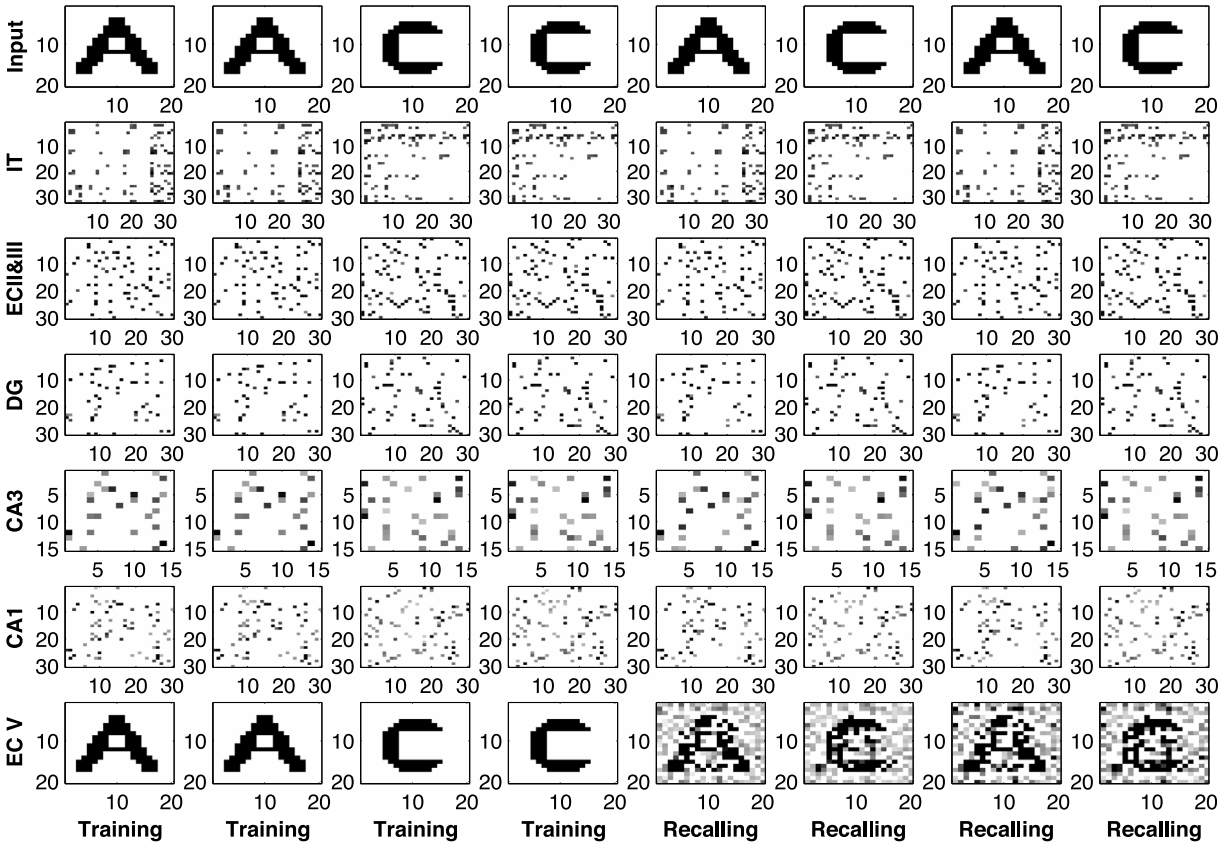

Fig. 5. Auto-associative property of the model. First two cycles are training for input image 'A', the next two cycles are training for input 'C'. Each cycle extends to the length of one theta cycle, to stabilize the neural responses to the input provided. In the testing stage image 'A' and 'C' are input to the system in alternate cycles. It is observed that the system is able, to some extent, to recall the learned patterns. Top to bottom: Each panel shows the input image, the mean firing rates of IT, ECII&III, DG, CA3, CA1 and ECV (Output) over one theta cycle for a single trial of the task.

2.3.2. Place-dependent property of CA1

According to Edelman's model (Edelman, 2007; Fleischer & Edelman, 2009), the CA1 region in the hippocampus shows a place-dependent response, i.e. certain neurons fire at certain robot locations. This place-dependent response was verified in an earlier work (Huang et al., 2014) by implementing the model in a mobile robot which is placed in a simulated plus-maze environment. A unique shape image is placed at the end of each arm of the maze to enable the robot to differentiate between different arms. When the robot moves to the end of the maze arm and looks at the image shown on the wall, the neuron activity in CA1 area shows different patterns for each maze arm. This place-dependent response is later seen in the current model as well (Section 3.1).

2.4. Experimental setup

Continuing the previous modeling studies on cognitive functions in spatial navigation, we are intrigued to answer the following questions:

1. In general, do the biologically-inspired models, in particular, the place-dependent response and neural mapping capabilities, enable any form of embodied cognitive navigation, i.e., can a robot embodied by these cognitive functions interact with its environment?
2. Can these neuro-cognitive models give rise to autonomous and adaptive behavior in the robot, similar to that of animals?

We developed a robotic hardware platform called NECO (Neuro-Cognitive Robot) based on the developed neural model and verified its cognitive navigation performance in a physical environment. We also used the simulated robotic platform developed in Huang et al. (2014) to further analyze the neuronal responses of our EC-Hippocampal model.

2.4.1. Experimental environment and task description

In the hardware implementation of the model, the task was to navigate a plus-maze and go to the desired arm using the NECO robot, both shown in Fig. 6 (Hardware details of the robotic platform are given in Appendix C). The maze is similar to the experiment performed with Darwin XI (Fleischer, Gally, Edelman, & Krichmar, 2007; Fleischer & Krichmar, 2007), which imitated the environment used in the studies of rodent hippocampal place activity Ferbinteanu and Shapiro (2003). At the start of each trial, the robot started from any arm of the maze, chosen at random. The robot had to make a choice of direction at the intersection, and traverse the chosen arm to the end. To provide visual cues for the robot, the wall at the end of each maze arm had a picture of an object on it, viz. an apple (labeled Apple), a piece of cheese (labeled Cheese), and a milk carton (labeled Milk).

Initially, to train the model, the robot was taken through to the end of three of the arms, until all neural regions showed sufficient activity. At the same time, they were given the expected values of ECV through the Task neurons, so that they could associate these values with the activities in the neural regions. After this, they were given tasks of navigating to the various learned objects. A task was assigned to the robot by providing an input in the appropriate neuron of the Task neural region. This was also extended to multiple tasks within the same trial, wherein many Task neurons were activated at once. Initially, single tasks were given to the

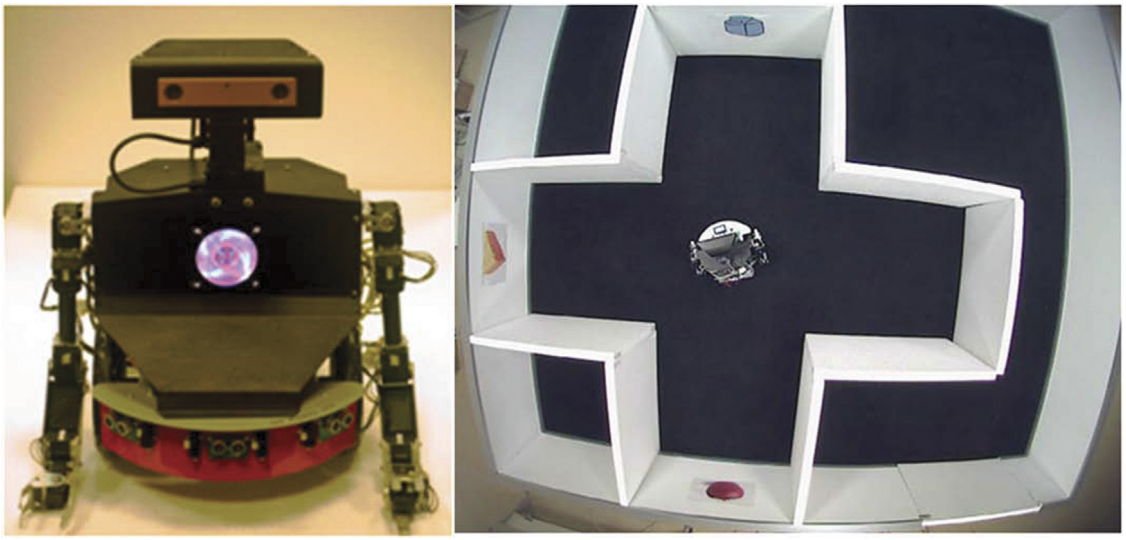

Fig. 6. The neuro-cognitive robot, NECO and an aerial view of the plus-maze environment. The maze has four arms with different shapes at each end to provide visual cues (shown here as Milk at the top of the image, Cheese on the left of the image and Apple at the bottom of the image). The camera and compass mounted on the robot head provide the vision and orientation inputs for the robot; the IR sensors on the base of robot are only used to detect the intersection.

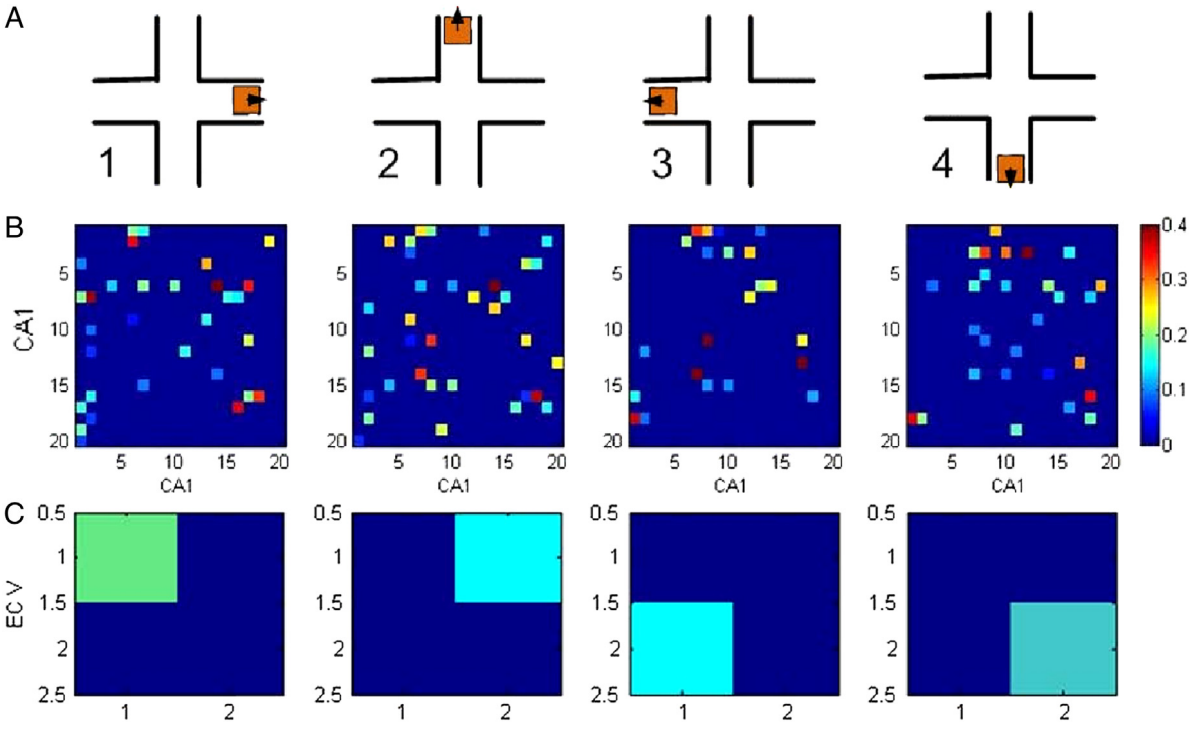

Fig. 7. Place-dependent patterns of CA1 and ECV at different locations during the learning phase. (A) The robot traverses the maze by navigating to the intersection, facing one of the arms and reaching the end of that arm—the arrow indicates the facing direction; (B) Each panel shows the mean firing rate of CA1 over one theta cycle after reaching the end of each arm. Different patterns for each arm correspond to a place-dependent response; (C) The neural response (mean firing rate) of ECV over one theta cycle after reaching the end of each arm. Each cell in ECV corresponds to the end of an arm, as shown earlier in Fig. 3.

robot; later, two tasks were given at the same time to test the multiple-task capabilities of the system.

2.4.2. Software simulation environment

To verify the working of the model and analyze neuronal activities, the neural model was first tested in a simulated robot. The simulation environment is developed in Webots, which is a dynamic simulation software based on Open Dynamic Engine (ODE). All the required real-world sensors such as the camera, compass, distance sensors, and DC motors to provide motion, can be modeled easily in this environment.

3. Experimental results and discussion

With the model described earlier, the mobile robot platform was able to achieve the cognitive navigation tasks assigned. The experimental results of the maze navigation can be found in our recorded video on Youtube:

"http://www.youtube.com/watch?v=iwI73cyBRac ".

The robot started off with visiting each maze arm in turn from left to right, where it saw, in order, pictures of Apple, Cheese and Milk. When learning each image, a Task neuron is seen to be activated, so that the corresponding ECV neuron is given a strong

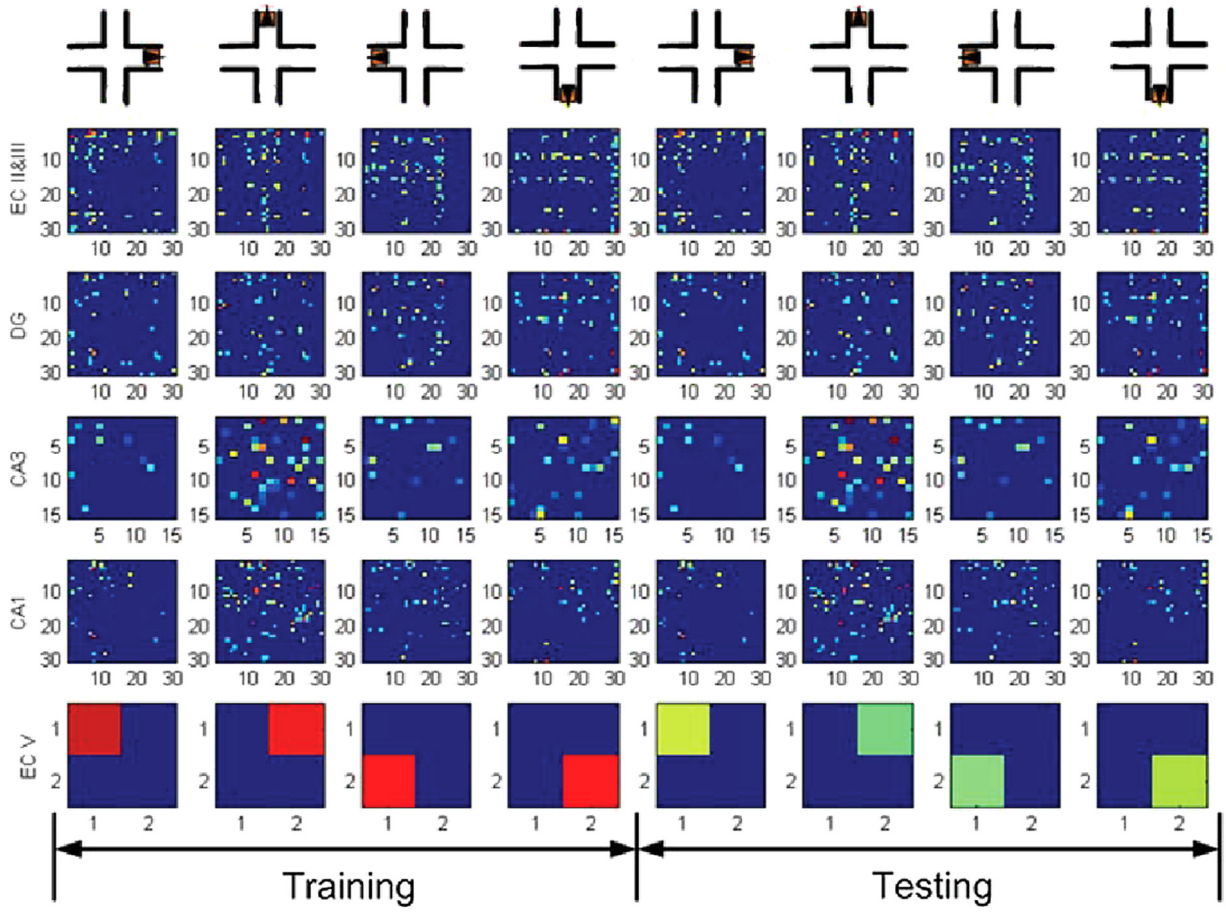

Fig. 8. Simulation results of neural mapping in plus-maze environment, after the robot traverses the length of each arm during training as well as testing. Top to bottom: Each panel shows the robot location in plus-maze, the mean firing rates of ECII&III, DG, CA3, CA1 and ECV over a theta cycle after reaching the end of each arm of the maze. During the training phase, when the robot has reached the end of an arm, a strong input is given to the appropriate neuron in the Task region, such that the corresponding neuron in ECV is strongly potentiated (represented here as a red shade). During the testing phase, when the robot has traversed an arm, a weak input from the appropriate Task neuron, along with the sensory information provided on reaching the end of the arm, is enough to potentiate the previously-learnt ECV neuron. (For interpretation of the references to color in this figure legend, the reader is referred to the web version of this article.)

input. In this experiment, Task neuron (1, 1) represents Apple, Task neuron (1, 2) represent Cheese, and Task neuron (2, 1) represents Milk.

After training of all images was done, the testing phase began. The first task given was to find Milk; this was done by providing input to the specified Task neuron (viz. (2, 1)). At the intersection, the robot looked once in all directions, to get input from each arm, and built up activity in the motor cortical area, Mhdg. In this case, the neural region in Mhdg corresponding to the Milk direction (right) was potentiated the most (owing to the connections formed between place-dependent activity in CA1, and EC V, which sends output to Mhdg). Hence, the robot chose to visit that direction and find Milk successfully. Similarly, the robot was asked to find Apple and Cheese in succession, and did so successfully.

The multiple-task phase was then started. The robot was asked to find Apple and Milk, by potentiating Task neurons (1, 1) and (2, 1). Two of the three arms it looked at contained both targets; between these, the robot chose Milk, as the Mhdg value in that direction happened to be higher. After visiting Milk, it was removed from the Task region, so as not to re-visit the same location again. The robot, now having only Apple left to visit, was able to navigate there using the same procedure. This experiment was repeated for other two-task combinations, namely Apple–Cheese, and Cheese–Milk.

The result shows that the robot was able to remember the locations it had previously visited, and go to them when requested.

3.1. Place-dependent response of CA1

In the learning phase of the experiment, when the robot moves to the end of a maze arm from the center, and looks at the image shown on the wall, the neuron activities in the CA1 area converge and reach a stable pattern after a single theta cycle (to stabilize the input). The neural activity pattern is different for each maze arm. This place-related pattern is shown in Fig. 7(B). In this place field response, about 57 neurons in total in CA1 area out of 400 neurons are fired when reaching all four different locations. The ratio is similar to the experimental results of Darwin XI (Fleischer & Krichmar, 2007). Since the CA1 area shows different patterns when the robot is placed in different arms, it is verified to have a place-dependent response, as posited earlier in Section 2.3.2. This property helps the robot to build a spatial encoding of the map in ECV area (as shown in Fig. 7(C)).

3.2. Spatial mapping property of EC

After training, the neurons in ECV were activated by the current location of the robot in the environment. Fig. 8 is the simulation result of neural mapping in the ECV to the plus-maze environment. During training, the ECV receives strong input from the Task region. This helps it associate the sensory input to the system, encoded as the place-dependent response of the CA1 region, with the coded location, via strengthening of the appropriate plastic connections

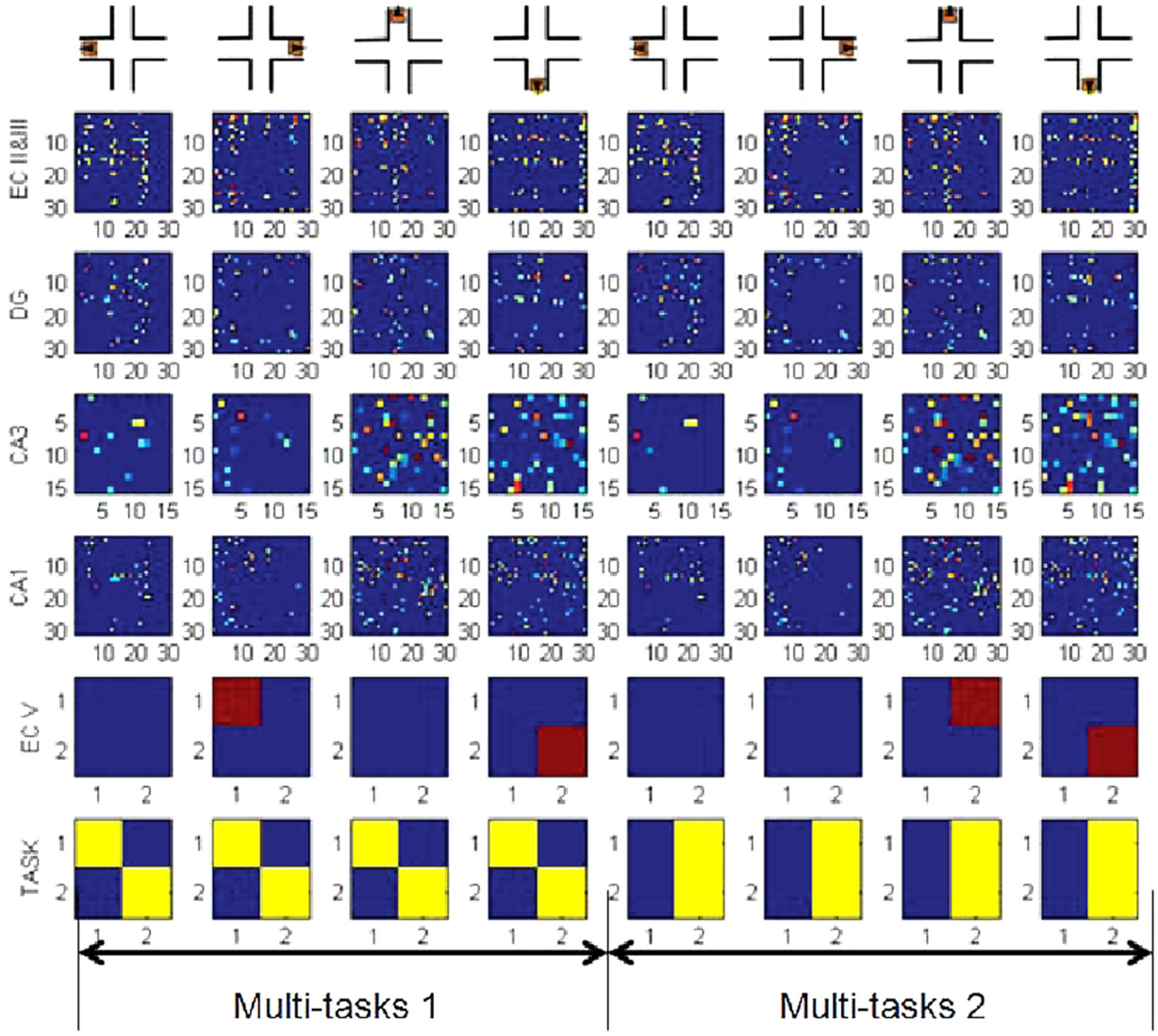

Fig. 9. Simulation results of the multi-task experiment, after the robot has traversed the length of each arm, for two different multiple-task scenarios. Top to bottom: Each panel shows the robot location in plus-maze, the mean firing rates of ECII&III, DG, CA3, CA1, ECV and Task regions over a theta cycle after reaching the end of each arm of the maze. It can be observed that the ECV region does not fire unless the corresponding neuron in the Task region has any input; in this case, it potentiates the ECV region enough to fire, which subsequently influences the Mhdg input (not shown here) to move in that direction. It should be noted that these are readings taken through the course of each multi-task experiment, and not indicative of the sequence of actions taken by the robot in finishing the task; this is merely to illustrate the difference between neural activities when multiple tasks are set for the robot.

from CA1 to itself. During the testing phase, the place-dependent response from CA1, combined with a weak input from the Task region, causes the ECV to have greater activity at that neuron.

Here, the odometric information and Task region are not shown. With the motion information, the robot can estimate the current location according to the initial point and associate it with the sensory inputs. This helps it explore the environment and build the map automatically for navigation.

3.3. Multi-task capability

The simulation results of the multi-task experiment are shown in Fig. 9. Similar to the previous single-task scenario, when the trained robot receives an input which matches the given task (i.e. the input from the Task region), the corresponding neuron in ECV would have an increased firing rate. This increase in activity would, in turn, boost the input to the Mhdg area, and allow the robot to make a decision to move to the desired target.

In the video for the third task starting at approximately 2:35 (find Cheese–Milk), it was observed that on the first try, the robot moves towards Cheese, even though both Milk and Cheese can be reached. Though both regions show higher activity in Mhdg, there are some random variations that may occur during the learning phase of any of the constituent regions. All other things being equal, these influence the robot to prefer one target to the other.

While currently it is hard to predict the order of target visitation because of these factors, we hope in the future to better study this and learn how to better predict the behavior of the model.

4. Conclusion

The hippocampus and the entorhinal cortex play important roles in spatial navigation. In this paper, we have presented our brain-inspired neural architecture for spatial navigation. The model includes three main layers — the neocortex, the entorhinal cortex, and the hippocampus, together with a hierarchical vision architecture and other sensory input cortical regions, and a motor output cortical region. This system allows us to track all the neural activities for different experiments. In the experiments, the place-dependent response and neural mapping property are shown to

Table 1
Information about the neural areas.

Area	Size	g	δ^{fire}	ω
V1color	6 × 8	1	0	0
V1shape	16 × 16	1	0	0
HD	1 × 360	1	0	0
IT	30 × 30	1	0.2	0.1
ITi	30 × 30	1	0.1	0.1
ANT	15 × 15	1	0.2	0.1
ANTi	15 × 15	1	0.1	0.1
Mhdg	1 × 60	1	0.1	0
Mhdgi	1 × 60	1	0	0
ECII&III	30 × 30	1	0.1	0.5
ECII&IIIi	30 × 30	1	0.02	0
ECV	2 × 2	1	0.1	0.5
ECVi	2 × 2	1	0.02	0
DG	30 × 30	0.75	0.1	0.5
DGi	30 × 30	1	0.02	0
CA3	15 × 15	0.75	0.05	0.5
CA3i	15 × 15	1	0.02	0
CA1	30 × 30	0.75	0.1	0.5
CA1i	30 × 30	1	0.02	0

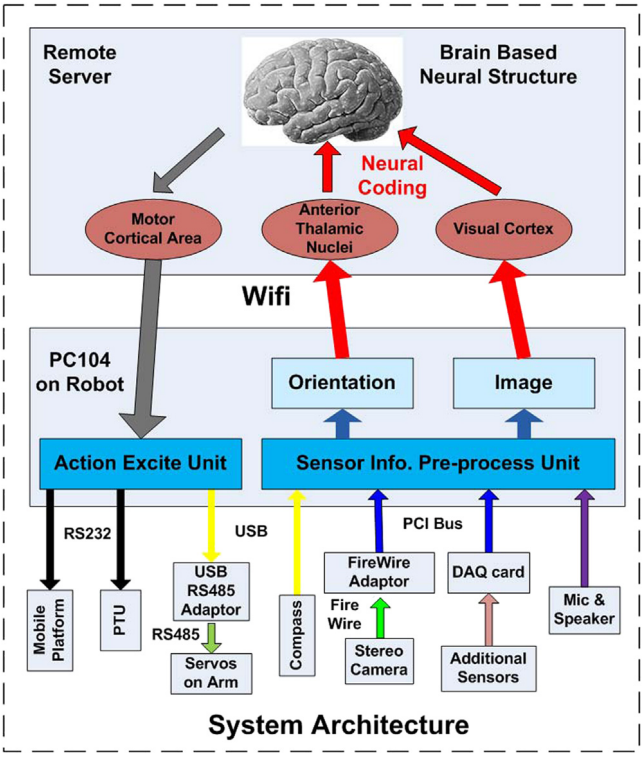

Fig. 10. Hardware structure of NECO.

be realized in the CA1 area of the hippocampus, and the entorhinal cortex, respectively. The robot is found to be able to remember the location of the goal that it had previously learnt. This exploratory study shows how the behavior of the hippocampus, in combination with a task-setting paradigm, can be used to contribute to navigation and spatial memory tasks in mobile robots.

Understanding how the cognitive functions of the brain arise from its basic physiological components is an enticing and challenging scientific frontier for many years, which requires not only the neural coding of internal cognitive constructs and the neural mechanisms of learning and memory, but also the representation of the external world (Burgess, 2014). The discoveries of place cells and grid cells have become a great achievement to answer this quest. Given this inspiration, this work and our other ongoing efforts (Hu, Tang, Tan, & Li, 2016; Yuan et al., 2015) are targeted at the cross disciplinary research of robotic cognition, which will contribute to decoding the neural representation of cognitive models exposed to the external world, and also to establishing new mapping and navigation models for robotics (Pfeifer, Lungarella, & Iida, 2007).

Acknowledgment

The last author's part of this work was supported by the National Natural Science Foundation of China under grant number 61673283.

Appendix A. Parameters of the simulated neural system

The simulated nervous system is modeled on the anatomy and physiology of the mammalian nervous system but, obviously, with far fewer neurons and a much less complex architecture. Each neural region contains neuronal units that can be either excitatory or inhibitory. In total, the simulated nervous system contained 19 neural areas, 9084 neuronal units, and approx 0.2 million synaptic connections. Specific parameters relating to each area and to patterns of connectivity are given in Tables 2 and 3. All these parameter values were initially taken from previous models (Huang et al., 2014), and tuned until they performed well for the current experiments.

In Table 1, the number of neuronal units and topology is shown in the size column. The other columns are physiological parameters for each neural area as defined in the simulation equations above. Roughly described, the parameters are scaling factor, g, firing rate threshold, δ^{fire}, and persistence factor, ω. This table includes inhibitory areas mentioned in Fig. 1.

Non-plastic connections between neural areas in the simulated nervous system are given in Table 2. A presynaptic neuronal unit connects to a postsynaptic neuronal unit with a given probability (P) and a given projection topology, as described in Section 2.2.2. The initial connection strengths are set with a basic strength and a variation range. A negative value of connection strength denotes inhibitory connections. ϕ denotes the persistence of the synapse. Some connections are special cases where the pre- and postsynaptic regions have different sizes, for example in the connection V1shape $\rightarrow$ IT, where IT is about double the size of V1shape. In these cases, the number of connecting neurons are scaled by the relative sizes of the regions. In the above case, one neuron in V1shape is connected to 4 neurons in IT, since it doubles in size along both width and height.

Plastic connections between neural areas in the simulated nervous system are shown in Table 3. A nonzero value of η, the learning rate parameter, signals a plastic connection that changes according to the modified BCM rule with parameters k_1 and k_2 in Eq. (6).

The number of steps required for reaching a stable state for a new input, N (as mentioned in Eq. (8)) was chosen to be 13.

Appendix B. Task region parameters

The Task region does not follow the regular neural dynamics of all other regions, since it is only introduced to provide training/testing boosts to the ECV. Its size is 2 × 2. It has a one-to-one mapping with ECV i.e. equivalent to a rectangular connection of size []1 × 1. It has a non-plastic connection of strength of 1 and probability 1. The input to Task is kept at 0.8 during training, and 0.3 for testing.

Appendix C. Hardware implementation details

Fig. 10 shows the details of the NECO mobile robotic platform used in our experiments. The robotic unit was 0.35 m in diameter

Table 2
Non-plastic connections between neural areas.

Projection direction	Projection topology	P	Basic strength	Variation	ϕ
V1color → IT	nontopo	0.05	0.05	0.02	1
V1shape → IT	[]1 × 1	0.5	0.6	0.2	1
HD → ANT	[]1 × 6	1	0.04	0.02	1
IT → ECII&III	[]1 × 1	1	0.2	0.1	1
IT → ITi	Θ1 × 2	1	0.06	0.02	1
ITi → IT	[]1 × 1	1	−0.5	0.14	1
ANT → ECII&II	[]1 × 1	1	0.3	0.1	1
ANT → ANTi	Θ1 × 2	0.25	0.01	0.01	1
ANTi → ANT	[]1 × 1	1	−0.5	0.14	1
ECII&III → ECV	nontopo	0.001	0.04	0.04	1
ECII&III → ECII&IIIi	Θ1 × 2	0.1	0.45	0.15	1
ECII&IIIi → ECII&III	[]1 × 1	1	−1.2	0.3	1
ECV → ECII&III	nontopo	0.001	0.04	0.04	1
ECV → Mhdg	nontopo	1	0.1	0.1	1
ECV → ECVi	Θ1 × 2	1	0.45	0.15	1
ECVi → ECV	[]1 × 1	1	−1.2	0.3	1
Mhdg → Mhdgi	Θ1 × 2	1	0.45	0.15	1
Mhdgi → Mhdg	[]1 × 1	1	−1.2	0.3	1
DG → DGi	Θ1 × 4	0.3	0.45	0.15	1
DGi → DG	[]1 × 1	1	−1.2	0.3	1
CA3 → CA3i	Θ1 × 2	0.1	0.45	0.15	1
CA3i → CA3	[]1 × 1	1	−1.2	0.3	1
CA1 → CA1i	Θ1 × 4	0.3	0.45	0.15	1
CA1i → CA1	[]1 × 1	1	−1.2	0.3	1
TR → ECII&III	nontopo	0.05	−0.02	0.01	1
TR → DG	nontopo	0.05	−0.02	0.01	1
TR → CA3	nontopo	0.05	−0.02	0.01	1
TR → CA1	nontopo	0.05	−0.02	0.01	1
TR → ECV	nontopo	0.05	−0.02	0.01	1

Table 3
Plastic connections between neural areas.

Projection direction	Projection type	P	B. S.	Var.	ϕ	η	k_1	k_2
ECII&III → DG	[]3 × 3	0.2	0.45	0.15	0.25	0.05	0.9	0.45
ECII&III → CA3	[]3 × 3	0.04	0.15	0.05	0.25	0.05	0.9	0.45
ECII&III → CA1	[]3 × 3	0.04	0.3	0.1	0.25	0.05	0.9	0.45
DG → CA3	[]3 × 3	0.06	0.45	0.15	0.25	0.05	0.9	0.45
CA3 → CA3	nontopo	0.01	0.02	0.01	0.25	0.05	0.9	0.45
CA3 → CA1	[]3 × 3	0.1	0.45	0.15	0.25	0.05	0.9	0.45
CA1 → ECV	nontopo	0.1	0.1	0.05	0.25	0.05	0.9	0.45

and 0.6 m in height. The processor of the robot was PC/104 with 2.26 GHz CPU speed. A stereo camera was mounted on a pan–tilt unit to provide visual input to the neural system. A magnetic compass provided heading input, and IR sensors were mounted on the front, left and right sides of the base to detect the maze intersection and walls.

References

Amaral, D. G., Ishizuka, N., & Claiborne, B. (1990). Neurons, numbers and the hippocampal network. In *Progress in brain research* (pp. 1–11). Amsterdam: Elsevier Science.

Barrera, A., & Weitzenfeld, A. (2006). Biological inspired neural controller for robot learning and mapping. In *Proc. IEEE int. joint conf. on neural networks, Vancouver* (pp. 3664–3671).

Bernard, C., & Wheal, H. V. (1994). Model of local connectivity patterns in CA3 and CA1 areas of the hippocampus. *Hippocampus*, *4*, 497–529.

Burgess, N. (2014). The 2014 nobel prize in physiology or medicine: a spatial model for cognitive neuroscience. *Neuron*, *84*(6), 1120–1125.

Cheu, E. Y., Yu, J., Tan, C. H., & Tang, H. (2012). Synaptic conditions for auto-associative memory storage and pattern completion in Jensen et al.'s model of hippocampal area CA3. *Journal of Computational Neuroscience*, *33*(3), 435–447.

Dissanayake, M., Newman, P., Clark, S., Durrant-Whyte, H. F., & Csorba, M. (2001). A Solution to the simultaneous localization and map building (SLAM) problem. *IEEE Transactions on Robotics and Automation*, *17*(3), 229–241.

Edelman, G. (2007). Learning in and from brain-based devices. *Science*, *318*, 1103–1105.

Ferbinteanu, J., & Shapiro, M. L. (2003). Prospective and retrospective memory coding in the hippocampus. *Neuron*, *40*(6), 1227–1239.

Fleischer, J., & Edelman, G. (2009). Brain-based devices. *IEEE Robotics & Automation Magazine*, *16*(3), 33–41.

Fleischer, J. G., Gally, J. A., Edelman, G. M., & Krichmar, J. L. (2007). Retrospective and prospective responses arising in a modeled hippocampus during maze navigation by a brain-based device. *Proceedings of the National Academy of Sciences*, *104*, 3556–3561.

Fleischer, J. G., & Krichmar, J. L. (2007). Sensory integration and remapping in a model of the medial temporal lobe during maze navigation by a brain-based device. *Journal of Integrative Neuroscience*, *6*(3), 403–431.

Frank, L. M., Brown, E. N., & Wilson, M. (2000). Trajectory encoding in the hippocampus and entorhinal cortex. *Neuron*, *27*, 169–178.

Fyhn, M., Molden, S., Witter, M. P., Moser, E. I., & Moser, M. B. (2004). Spatial representation in the entorhinal cortex. *Science*, *305*, 1258–1264.

Hafting, T., Fyhn, M., Molden, S., Moser, M. B., & Moser, E. I. (2005). Microstructure of a spatial map in the entorhinal cortex. *Nature*, *436*(11), 801–806.

Hargreaves, E. L., Rao, G., Lee, I., & Knierim, J. J. (2005). Major dissociation between medial and lateral entorhinal input to dorsal hippocampus. *Science*, *308*, 1792.

Hu, J., Tang, H., Tan, K. C., & Li, H. (2016). How the brain formulates memory: a spatio-temporal model. *IEEE Computational Intelligence Magazine*, *11*(2), 56–68.

Huang, W., Tang, H., & Tian, B. (2014). Vision enhanced neuro-cognitive structure for robotic spatial cognition. *Neurocomputing*, *129*, 49–58.

Kesner, R. P., Lee, I., & Gilbert, P. (2004). A behaviour assessment of hippocampal function based on a subregional analysis. *Reviews in the Neurosciences*, *15*, 331–335.

Krichmar, J. L., Nitz, D. A., Gally, J. A., & Edelman, G. M. (2004). Characterizing functional hippocampal pathways in a brain-based device as it solves a spatial memory task. *Proceedings of the National Academy of Sciences*, *102*, 2111–2116.

Lavenex, P., & Amaral, D. G. (2000). Hippocampal neocortical interaction: a hierarchy of associativity. *Hippocampus*, *10*, 420–430.

Martin, S. J., Grimwood, P. D., & Morris, R. G. M. (2000). Synaptic plasticity and memory: an evaluation of the hypothesis. *Annual Review of Neuroscience*, *23*, 649–711.

McNaughton, B. L., Battaglia, F. P., Jensen, O., Moser, E. I., & Moser, M. B. (2006). Path integration and the neural basis of the 'cognitive map'. *Nature Reviews Neuroscience*, *7*, 663–678.

Montemerlo, M., & Thrun, S. (2003). Simultaneous localization and mapping with unknown data association using FastSLAM. In *Proc.IEEE international conference on robotics and automation, ICRA* (pp. 1985–1991).

O'Keefe, J., & Dostrovsky, J. (1971). The hippocampus as a spatial map. Preliminary evidence from unit activity in the freely-moving rat. *Brain Research*, *34*(1), 171–175.
O'Keefe, J., & Nadel, L. (1978). *The Hippocampus as a cognitive map*. Oxford University Press.
Pfeifer, R., Lungarella, M., & Iida, F. (2007). Self-organization, embodiment, and biologically inspired robotics. *Science*, *318*, 1088–1093.
Riesenhuber, M., & Poggio, T. (1999). Hierarchical models of object recognition in cortex. *Nature Neuroscience*, *2*(11), 1019–1025.
Shim, V. A., Ranjit, C. S. N., Tian, B., Yuan, M., & Tang, H. (2015). A simplified cerebellar model with priority-based delayed eligibility trace learning for motor control. *IEEE Transactions on Autonomous Mental Development*, *7*(1), 26–38.
Shim, V.A., Tian, B., Yuan, M., Tang, H., & Li, H. (2014). Direction-driven navigation using cognitive map for mobile robots. In *Proc. of 2014 IEEE/RSJ international conference on intelligent robots and systems, IROS, Chicago, USA* (pp. 2639–2646).
Tang, H., Li, H., & Yan, R. (2010). Memory dynamics in attractor networks with saliency weights. *Neural Computation*, *22*, 1899–1926.
Thrun, S., Burgard, W., & Fox, D. (2005). *Probabilistic robotics (intelligent robotics and autonomous agents)*. The MIT Press.
Tian, B., Shim, V.A., Yuan, M., Srinivasan, C., Tang, H., & Li, H. (2013). RGB-D based cognitive map building and navigation. In *Proc. of 2013 IEEE/RSJ international conference on intelligent robots and systems, IROS, Tokyo, Japan* (pp. 1562–1567).
Treves, A., & Rolls, E. T. (1994). Computational analysis of the role of the hippocampus in memory. *Hippocampus*, *4*, 374–391.
Treves, A., & Rolls, E. T. (1994). Computational analysis of the role of the hippocampus in memory. *HIPPOCAMPUS*, *4*(3), 374–391.
Ungerleider, L. G., & Haxby, J. V. (1994). "What" and "Where" in the human brain. *Current Opinion in Neurobiology*, *4*, 157–165.
Wyeth, B. G., & Milford, M. (2009). Spatial cognition for robots. *IEEE Robotics & Automation Magazine*, *16*(3), 24–32.
Yuan, M., Tian, B., Shim, V.A., Tang, H., & Li, H. (2015). An entorhinal-hippocampal model for simultaneous cognitive map building. In *Proceedings of the 29th AAAI conference on artificial intelligence, AAAI-15, Austin, TX, USA* (pp. 586–592).